# Reaction and Diffusion during Demineralization of Animal Bone

**Danielle A. Horneman, Marcel Ottens, Marieke Hoorneman, and Luuk A. M. van der Wielen**
Dept. of Biotechnology, Delft University of Technology, 2628 BC, Delft, The Netherlands

**Martijn Tesson**
Delft Gelatin BV, P.O. Box 3, 2600 AA, Delft, The Netherlands

*DOI 10.1002/aic.10264*
*Published online in Wiley InterScience (www.interscience.wiley.com).*

*The demineralization of animal bone is investigated. Experimental results show an increase in penetration rate of hydrochloric acid into animal bone particles, and thereby increased demineralization, at increasing temperature and concentration of HCl. Fick's law is used to calculate the effective diffusivities of HCl in animal bone from these experimental results, showing a decrease in effective diffusivity at increased HCl concentration, which proves Fick's law unsuitable for describing the process, whereas a Maxwell–Stefan-based model is used successfully. This model is able to take into account gradients in composition as well as electrical potential, and also addresses the frictional resistances between the various components in the multicomponent system. The results of the Maxwell–Stefan model are in good agreement with the experimental data. From the Maxwell–Stefan model and the experiments, it follows that at high concentrations of HCl, the friction between the diffusing ions ($H^+$, $Cl^-$, $H_2PO_4^-$, and $Ca^{2+}$) becomes more important and lowers the increase of demineralization rate caused by the increase in the concentration gradient.* © 2004 American Institute of Chemical Engineers *AIChE J,* 50: 2682–2690, 2004

*Keywords: multicomponent diffusion, Maxwell–Stefan, modeling, shrinking core model, gelatin production, demineralization, porous media*

## Introduction

Gelatin is an important material, finding application in the food, pharmaceutical, and photographic industries. It is a high molecular weight polypeptide obtained by the partial hydrolysis of collagen. Collagen is distinctive among proteins because it contains an unusually high level of two cyclic amino acids, hydroxyproline and proline (Babel et al., 2000; Rose, 1987). One of the important properties of gelatin is the thermally reversible gel formation. This is a relatively unique feature among proteins (Babel et al., 2000; Rose, 1987).

The raw materials used in conventional gelatin production are cattle bones, cattle hides, and pork skin. The characteristics of these gelatins vary from batch to batch, which is unwanted especially for medical and photographic applications. Recombinant gelatins produced in microbial cells give gelatin with a reproducible quality and seems to be a good alternative (Werten et al., 1999, 2001). For now, gelatin is mainly produced in the conventional way. Outside the United States, cattle bones are one of the most important sources for collagen (Babel et al., 2000). Before the hydrolysis of collagen in the bones, all noncollagen compounds have to be removed. First, the bones are cleaned, degreased, dried, classified by size, and crushed. The resulting bone particles are contacted with a dilute acid, usually hydrochloric acid (Babel et al., 2000; Makarewicz et al., 1980), to remove the mineral salts. The

Correspondence concerning this article should be addressed to L. A. M. van der Wielen at L.A.M.vanderWielen@TNW.TUDelft.nl.

**Table 1. Diameter Distribution of the Different Types of Bones**

| Bone Type | Mass Fraction (wt %) | | | | |
|---|---|---|---|---|---|
| | $d_p > 11.2$ mm | $8 < d_p < 11.2$ mm | $5.6 < d_p < 8$ mm | $4 < d_p < 5.6$ mm | $d_p < 4$ mm |
| I | 0 | 2 | 48.7 | 45.04 | 4.26 |
| II | 18.6 | 58.0 | 21.3 | 1.95 | 0.15 |
| III | 0 | 1.5 | 35.8 | 51.57 | 11.23 |
| IV | 12.8 | 57 | 27.9 | 4.6 | 0.53 |

principal noncollagen component of the bone matrix is the mineral salt tricalcium phosphate [$Ca_3(PO_4)_2$], but also calcium carbonate ($CaCO_3$) is present (Makarewicz et al., 1980). The demineralization process is described by the following stoichiometric equations

$$Ca_3(PO_4)_2^{S} + 4\,HCl^{L} \rightarrow Ca(H_2PO_4)_2^{L} + 2\,CaCl_2^{L} \quad (1)$$

$$CaCO_3^{S} + 2\,HCl^{L} \rightarrow CO_2^{G} + H_2O^{L} + CaCl_2^{L} \quad (2)$$

where subscripts S, L, and G indicate the solid, liquid, and vapor state, respectively. Hydrochloric acid (HCl) diffuses into the bone particles and reacts with $Ca_3(PO_4)_2$ and $CaCO_3$ to form monocalcium phosphate [$Ca(H_2PO_4)_2$] and calcium chloride ($CaCl_2$), which are both soluble in the acid stream, and carbon dioxide, which leaves the process as a gas. The diffusion of HCl into the bone matrix is considered to be the rate-limiting step in the demineralization of bone. A qualitative and quantitative understanding of this diffusion process seems a route to increase the productivity of the demineralization process.

The mechanism of the demineralization process was investigated by Makarewicz et al. (1980) for the case of hard bone particles. Hard bone particles are almost uniform in density and structure, whereas porous bone particles, coming from the inner bone sections and joints, are less uniform in density and contain cavities. Makarewicz calculated the diffusivities in these hard bone particles using Fick's law to describe the mass transfer, although this method is not suitable for predicting the demineralization rate.

The aim of this study is to obtain more quantitative insight into the diffusion behavior of hydrochloric acid into bone particles, to improve the existing gelatin production process. Therefore an experimental program is performed to determine the influence of acid concentration, temperature, and bone structure properties, such as density, on the rate of demineralization. Both Fick's law and the Maxwell–Stefan model are tested on their ability to describe the mass transfer process during demineralization.

## Materials and Methods

The degreased and size-reduced pieces of cattle bones were obtained from the production line of gelatin at Delft Gelatin just before entering the demineralization unit. These bone particles are classified into four fractions, with properties given in Tables 1 and 2.

Before each experiment, the density of the bones was determined by measuring the increase in volume after placing a certain weight of bone particles in a known volume of ethanol. Ethanol was used because of its better wetting characteristics for bone than water and its lower density relative to that of water.

HCl, obtained from the storage tanks at Delft Gelatin (15 wt %), was used to make the solutions for the experiments (0.5, 3, or 6 wt %). The exact concentration of each solution was measured by determination of the equivalence point by titration with sodium hydroxide after addition of methyl red.

A general experimental procedure was used to measure the penetration depth of HCl into bone particles as a function of time.

Bone particles were kept in demineralized water overnight to prewet the particles. The demineralization experiment was started by placing the bone particles in an HCl solution of 0.5, 3, or 6 wt %. The mass ratio of bone to HCl solution was taken such that the concentration of HCl would remain approximately constant during the demineralization. The total amount of HCl needed to demineralize all the bones was calculated. This number was multiplied by 5 to keep the HCl concentration constant during the experiment. During the experiment, the temperature of the solution was kept constant by means of a thermostated bath.

To measure the penetration depth of HCl as a function of time, samples of about two to four bone particles were removed from the HCl solution. The bone particles were washed with demineralized water and frozen in a small volume of demineralized water. The frozen particles are sawed into two parts with an electric sawing machine (Kinzo 8E205). Freezing the bone particles is necessary to prevent deformation of the demineralized layer during the sawing process. The frozen water also dissipates the heat generated during sawing (Makarewicz et al., 1980). Under a visual light microscope, the demineralized layer of the bone particle is visible (see Figure 1) and the penetration depth was measured.

The experiments were performed at various temperatures, various acid concentrations, and with the bone types as shown in Table 3.

## Theory

### *The unreacted shrinking core model*

To describe the demineralization process, some general assumptions were made. First, the demineralization is limited by

**Table 2. Properties of the Different Types of Bones**

| Bone Type | $x_{moisture}$ (g/g) | $x_{phosphate}$ (g/g) | Density (kg/m$^3$) |
|---|---|---|---|
| I | 0.115 | 0.241 | $2.1 \times 10^3 \pm 77$ |
| II | 0.107 | 0.237 | $2.0 \times 10^3 \pm 77$ |
| III | 0.142 | 0.207 | $1.7 \times 10^3 \pm 78$ |
| IV | 0.118 | 0.201 | $1.7 \times 10^3 \pm 77$ |

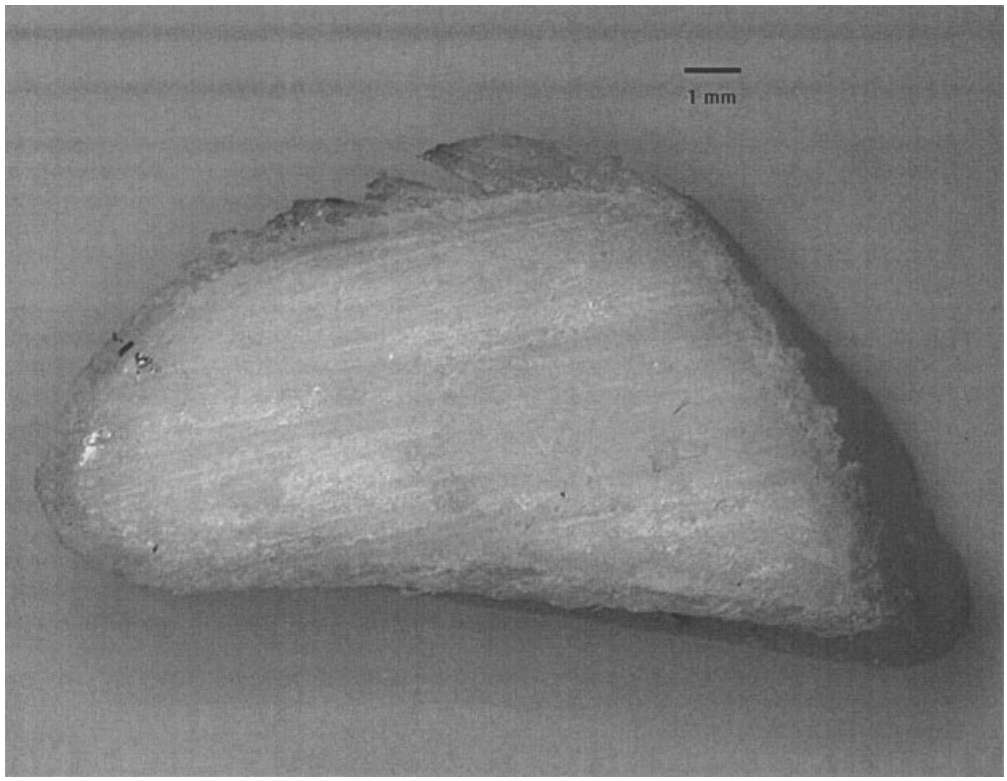


**Figure 1. Partly demineralized bone particle.**

The picture was taken after 4 h of demineralization in 6 wt % HCl at 10°C.

internal diffusion with reactions 1 and 2 being instantaneous and complete (Croome and Clegg, 1965; Makarewicz et al., 1980). Second, the demineralization process does not influence the size and the shape of the bone particles. In this way, a growing demineralized layer is formed around an unreacted core separated by a sharp reaction front (Makarewicz et al., 1980). This is described by the unreacted shrinking core model (Levenspiel, 1972; Westerterp et al., 1987).

**Table 3. Overview of the Experimental Conditions**

| Experiment | Bone Type | $C_{HCl}$ (wt %) | $T$ (°C) |
|---|---|---|---|
| I(0.5, 10) | I | 0.5 | 10 |
| I(0.5, 15) | I | 0.5 | 15 |
| I(3, 10) | I | 3 | 10 |
| I(3, 15) | I | 3 | 15 |
| I(6, 10) | I | 6 | 10 |
| I(6, 15) | I | 6 | 15 |
| II(0.5, 15) | II | 0.5 | 15 |
| II(3, 10) | II | 3 | 10 |
| II(3, 15) | II | 3 | 15 |
| II(3, 18) | II | 3 | 18 |
| II(6, 10) | II | 6 | 10 |
| II(6, 15) | II | 6 | 15 |
| II(6, 18) | II | 6 | 18 |
| II(6, 21) | II | 6 | 21 |
| III(3, 10) | III | 3 | 10 |
| III(3, 15) | III | 3 | 15 |
| III(6, 10) | III | 6 | 10 |
| III(6, 15) | III | 6 | 15 |
| IV(3, 10) | IV | 3 | 10 |
| IV(3, 15) | IV | 3 | 15 |
| IV(6, 10) | IV | 6 | 10 |
| IV(6, 15) | IV | 6 | 15 |

### *Diffusion described by Fick's law*

The flow of HCl, $J_{HCl}$, diffusing into the bone particle described by Fick's first law, reads

$$J_{HCl} = -4\pi r^2 D \frac{dC_{HCl}(r, t)}{dr} \tag{3}$$

where $D$ is Fick's effective diffusivity of HCl in the demineralized layer and $r$ is the radial position in the bone particle (Figure 2). The first assumption indicates that the concentration

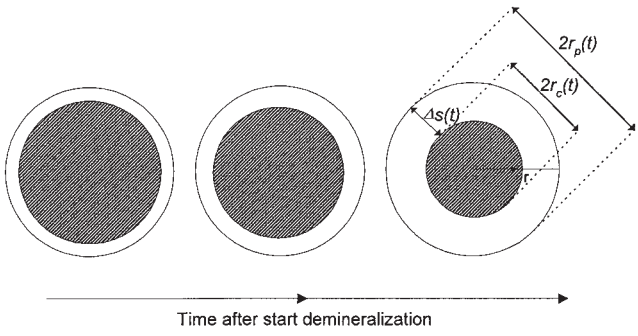


**Figure 2. Representation of the demineralization of bone particles.**

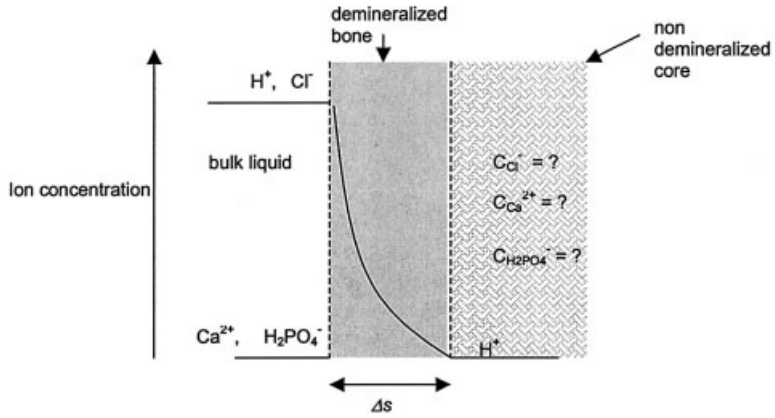


**Figure 3. Overview of the known concentrations of the ions in a bone particle during demineralization.**

of HCl at the boundary of the unreacted core ($r = r_c$) can be neglected. Integration of Eq. 3 from $r = r_p$ to $r = r_c$ at time $t$ thus gives

$$J_{\mathrm{HCl}} = -4\pi D C_{\mathrm{HCl}}(r_p, t)\frac{r_p r_c}{r_p - r_c} \tag{4}$$

where $r_p$ is the diameter of the bone particle and $r_c$ is the diameter of the unreacted core. The concentration of HCl at $r = r_p$ is equal to the concentration in the bulk liquid.

The molar flux of HCl into the demineralized layer is also equal to the amount of HCl that reacts at the reaction front (Westerterp et al., 1987)

$$J_{\mathrm{HCl}} = -\lambda 4\pi r_c^2 \frac{dr_c}{dt} \tag{5}$$

where $\lambda$ is the amount of moles of HCl needed to demineralize 1 $m^3$ of bone particles. To calculate this parameter, it is assumed that reaction 1 (Eq. 1) is the major demineralization reaction (Makarewicz et al., 1980). The amount of HCl needed is then approximately the stoichiometric amount of HCl needed to demineralize 1 $m^3$ of bone particles.

Combining Eqs. 4 and 5 yields a relation for the rate of change in the core diameter

$$\frac{dr_c}{dt} = \frac{DC_{\mathrm{HCl}}}{\lambda}\frac{r_p}{r_p r_c - r_c^2} \tag{6}$$

Integration of this relation gives a relation of the unreacted core diameter as a function of time

$$t = \frac{\lambda r_p^2}{6DC_{\mathrm{HCl}}}\left[1 - 3\left(\frac{r_c}{r_p}\right)^2 + 2\left(\frac{r_c}{r_p}\right)^3\right] \tag{7}$$

Rearrangement of Eq. 7 and replacing $r_p - r_c$ by the thickness of the demineralized layer ($\Delta s$) gives the following relation for $\Delta s$ as function of time

$$\Delta s = \sqrt{\frac{6DC_{\mathrm{HCl}} r_p t}{\lambda(3r_p - 2\Delta s)}} = K_{\mathrm{F}}\sqrt{t} \tag{8}$$

For small values of $\Delta s$ Eq. 8 is the same as that derived by Makarewich and coworkers in the case of diffusion into a planar semi-infinite plate (Makarewicz et al., 1980). A plot of $\Delta s$ as function of time will also provide information about the constant $K_{\mathrm{F}}$ and thus about the effective diffusivity of HCl.

### *Mass transfer described by Maxwell–Stefan model*

Fick's law gives good predictions for mass transfer in binary mixtures with a concentration gradient as the only driving force. There are, however, many other situations possible such as multicomponent mixtures and mixtures in heterogeneous media. In these situations friction will occur between each pair of components, including any solid matrix. There are also situations where other driving forces occur, such as electrical and pressure gradients. In all these situations, Fick's law does not always describe mass transfer well. The Maxwell–Stefan model, which overcomes the aforementioned limitations, is a general approach to describe mass transfer in many more situations. It relates the driving forces for transport to the encountered frictional resistance (Wesselingh and Krishna, 2000).

Demineralization of animal bones is a process involving a multicomponent mixture. It contains different ions, a porous solid phase, and water. Because of the movements of the ions there may be an electrical gradient in addition to the concentration gradient. Further, frictional resistances exist between the ions, water, and the solid matrix, which in this case is the demineralized layer.

The demineralization can be described by the reaction equations given in the introduction. It is assumed that $CO_2$ will leave the system immediately. This means that there are six components to take into account: the ions $H^+$ (1), $Cl^-$ (2), $H_2PO_4^-$ (3), and $Ca^{2+}$ (4); (5) water ($w$); and (6) the solid matrix ($M$). We regard the solid matrix as separate and assume that the water is stagnant. The transport of each ion can then be described by the following flux equation (Wesselingh and Krishna, 2000)

$$-\frac{\Delta x_i}{x_i} - \frac{Fz_i\Delta\phi}{RT} = \left(\frac{N_i}{Đ_{iM}} + \frac{N_i}{Đ_{iw}} + \sum_{j\neq i}\frac{x_j N_i - x_i N_j}{Đ_{ij}}\right)\frac{\Delta s}{x_i c} \tag{9}$$

where $F$ is the Faraday constant, $R$ is the gas constant, and $T$ is the temperature. The left-hand term describes the driving forces

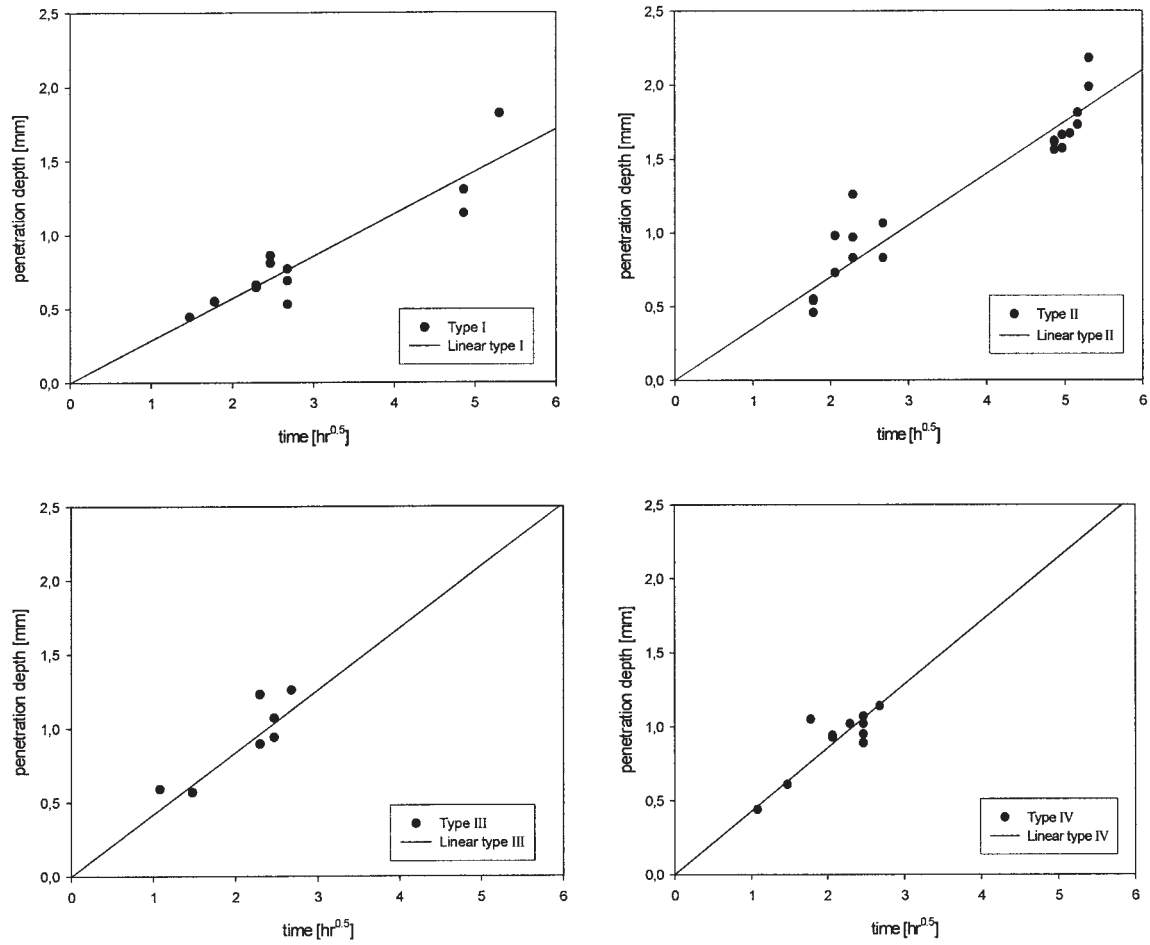


**Figure 4. Example of the penetration depth vs. time measured at $C_{HCl}$ = 6 wt % and $T$ = 10°C.**

where $x_i$ is the molar fraction of component $i$, $z_i$ is the charge of the component, and $\Delta\phi$ is the electrical potential gradient. The right-hand term of this equation describes the encountered frictional resistance of ion $i$ with the matrix ($M$), water ($w$), and the other ions. $N_i$ is the molar flux of ion $i$ in mol/m$^2$s and $Đ_{ij}$ is the Maxwell–Stefan diffusivity of component $i$ in $j$.

To solve the transport equations, the diffusivities have to be known. The diffusivities of the ions in water, $Đ_{iw}$, are taken from the literature (Mills et al., 1989) and are corrected for the viscosity with the modified Stokes–Einstein relation of Versteeg (Versteeg and Swaaij, 1983)

$$\frac{Đ_{ref}}{Đ} = \left(\frac{\eta}{\eta_{ref}}\right)^{0.6} \tag{10}$$

The diffusivities of the ions into the solid particle, $Đ_{iM}$, are estimated using the Ogston model (Bosma and Wesselingh, 2000

$$Đ_{iM} = Đ_{iw}\exp\left[-\sqrt{\ln\left(\frac{1}{1-\phi_f}\right)\left(1+\frac{r_i}{r_f}\right)^2}\right] \tag{11}$$

**Table 4. Experimentally Found $K_F$ Values***

| Exp. | $K_F$ (mm/h$^{-1/2}$) | Exp. | $K_F$ (mm/h$^{-1/2}$) | Exp. | $K_F$ (mm/h$^{-1/2}$) | Exp. | $K_F$ (mm/h$^{-1/2}$) |
|---|---|---|---|---|---|---|---|
| I(0.5, 10) | 0.14 | | | | | | |
| I(0.5, 15) | 0.12 | II(0.5, 15) | 0.14 | | | | |
| I(3, 10) | 0.24 | II(3, 10) | 0.28 | III(3, 10) | 0.35 | IV(3, 10) | 0.37 |
| I(3, 15) | 0.31 | II(3, 15) | 0.30 | III(3, 15) | 0.43 | IV(3, 15) | 0.42 |
| | | II(3, 18) | 0.30 | | | | |
| | | II(3, 21) | 0.34 | | | | |
| I(6, 10) | 0.29 | II(6, 10) | 0.35 | III(6, 10) | 0.43 | IV(6, 10) | 0.43 |
| I(6, 15) | 0.37 | II(6, 15) | 0.38 | III(6, 15) | 0.50 | IV(6, 15) | 0.53 |
| | | II(6, 18) | 0.40 | | | | |
| | | II(6, 21) | 0.41 | | | | |

*All $K_F$ values have an error of ±0.01.

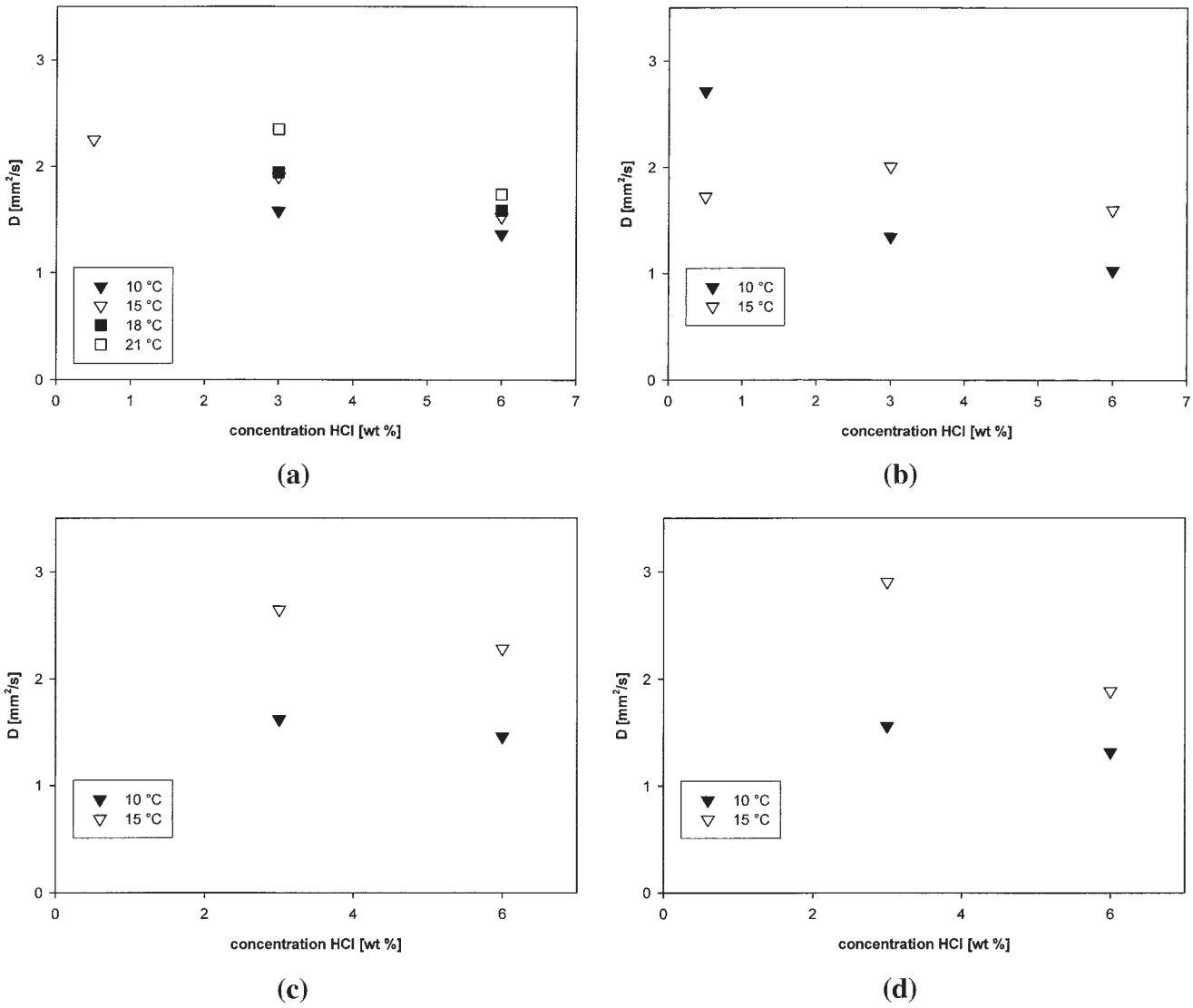


**Figure 5. Fickian diffusivity of HCl as function of concentration ($\Delta s$ = 0.1 cm).**

(a) Bone type I, (b) bone type II, (c) bone type III, (d) bone type IV.

where $r_i$ is the radius of the ion and $\phi_f$ is the solid volume fraction in the demineralized layer. The radius of the collagen fibers, $r_f$, is about 0.45 nm (Rose, 1980).

For the cation–anion diffusivities, we have used the following empirical relation (Krishna, 1987)

$$Đ_{\pm} = 4.8 \times 10^8 Đ^{\infty}_{+w} Đ^{\infty}_{-w} \frac{I_x^{0.55}}{|z_+ z_-|^{1.85}} \tag{12}$$

where $Đ^{\infty}_{+w}$ and $Đ^{\infty}_{-w}$ are the intrinsic diffusivities of the cation and ion, respectively, in water. $I_x$ is the mole fraction based ionic strength of the electrolyte solution.

The diffusivities of ions with like charge are taken from the literature (Wesselingh et al., 1995).

To calculate the fluxes, the molar fractions of each ion have to be known. Because of the high mass ratio of HCl to bone particles, the concentration of $H^+$ in the bulk liquid is relatively constant during the demineralization and equals the concentration of HCl in the bulk liquid. For the same reason the concentration of $Ca^{2+}$ and $H_2PO_4^-$ will be almost zero in the bulk liquid, which means that the concentration of $Cl^-$ approximately equals to that of $H^+$. At the reaction plane of the demineralized layer only the proton concentration is known, which equals 0 according to the first assumption. Figure 3 gives an overview of this situation.

Additional relations are required to calculate the fluxes: the unknown concentrations and the electrical potential gradient $\Delta\phi$. The first relation is the electroneutrality equation (Wesselingh and Krishna, 2000)

$$\sum z_i x_i = 0 \tag{13}$$

By using this equation it is assumed that the charge separation is negligible. The second relation is the no-current relation (Wesselingh and Krishna, 2000)

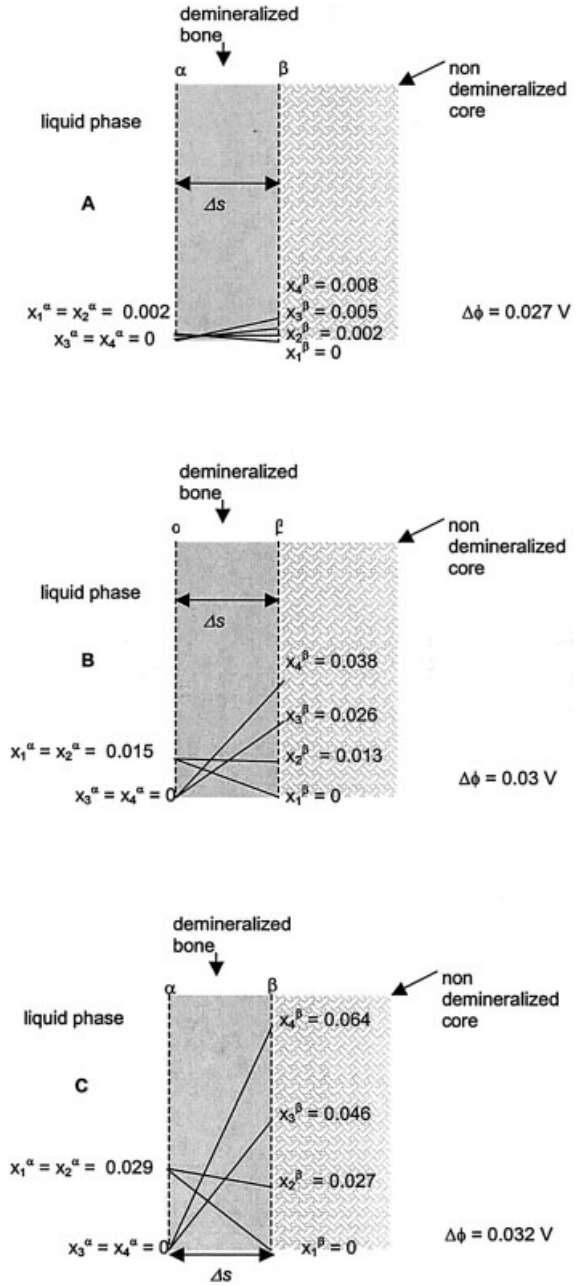


**Figure 6. Molar fraction of the components in the liquid phase ($\alpha$) and at the boundary between the demineralized layer and the unreacted core ($\beta$) during the demineralization of bone type I at different HCl concentrations in the liquid.**

(A) 0.5 wt % HCl, (B) 3 wt % HCl, (C) 6 wt % HCl.

$$\sum z_i N_i = 0 \tag{14}$$

Finally, there are two relations, based on the reaction stoichiometry of the demineralization, as follows

$$N_2 = \beta_2 N_1$$

$$N_3 = \beta_3 N_1 \tag{15}$$

where $\beta_i$ is the stoichiometric coefficient in moles $i$ per mole $Ca_3(PO_4)_2$. This yields a system of eight equations and eight unknowns. Thus, by using Eqs. 9 to 15 it is now possible to calculate all the fluxes and concentrations for different values of $\Delta s$.

To compare the outcome of the Maxwell–Stefan theory with the experiments, a relation is needed that describes the thickness of the demineralized layer as a function of time. The rate of change of the thickness of demineralized layer is given by

$$\frac{d\Delta s}{dt} = \frac{N_1}{\lambda} \tag{16}$$

Filling in the transport relation for $H^+$ (Eq. 9) and integration gives

$$\Delta s = \sqrt{\frac{2x_1 c\left(\dfrac{-\Delta x_1}{x_1} - \dfrac{Fz_1\Delta\phi}{RT}\right)}{\lambda\left(\dfrac{1}{Đ_{1M}} + \dfrac{1}{Đ_{1w}} + \displaystyle\sum_{j\neq 1}\dfrac{x_j - x_1\dfrac{\beta_j}{\beta_1}}{Đ_{1j}}\right)}}\, t = K_{MS}\sqrt{t} \tag{17}$$

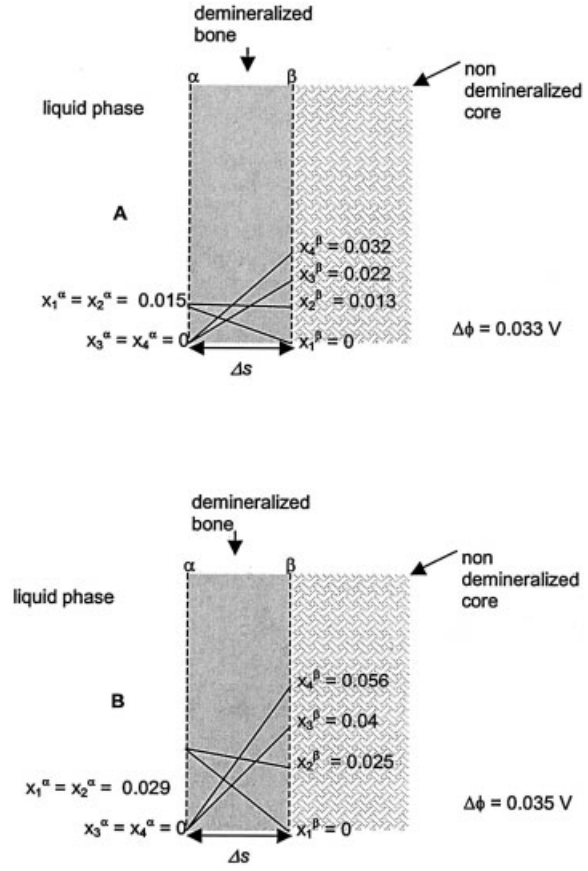


**Figure 7. Molar fraction of the components in the liquid phase ($\alpha$) and at the boundary between the demineralized layer and the unreacted core ($\beta$) during the demineralization of bone type IV at different HCl concentrations in the liquid.**

(A) 3 wt % HCl, (B) 6 wt % HCl.

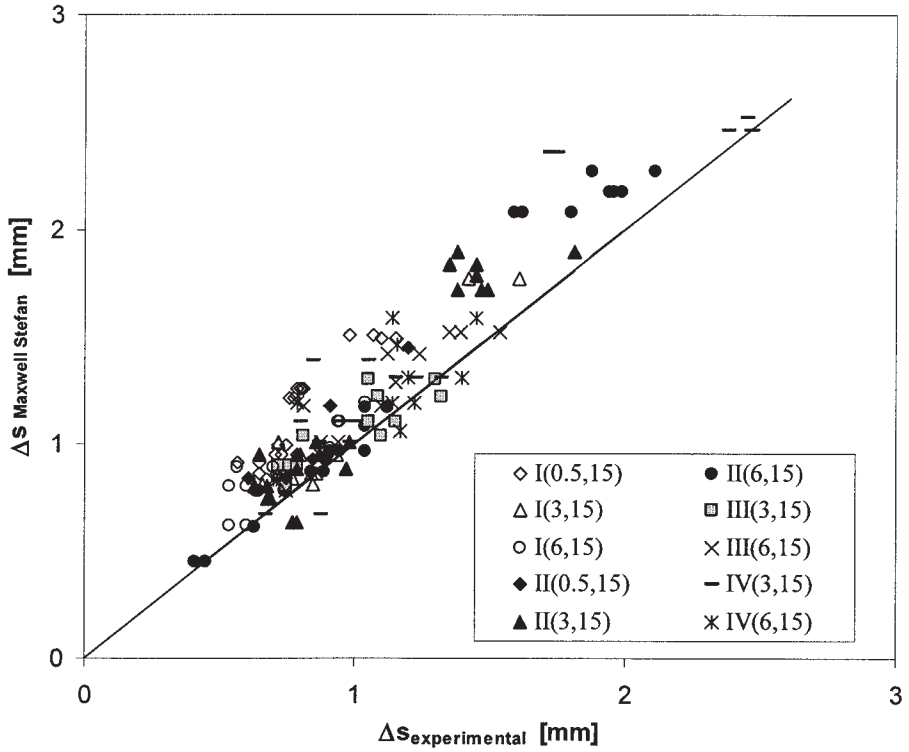


**Figure 8. Parity plot of predicted penetration depth and the experimental penetration depth.**

where $K_{MS}$ is a parameter that gives an indication of the demineralization rate.

## Results and Discussion

### *Penetration in the different types of bone particles*

The penetration depth is plotted vs. the square root of time. Figure 4 shows a selection of these plots. By inspection of Figure 4, it shows that the rate of demineralization in the two porous types of bones, types III and IV, is much faster than the demineralization of the two other types of bone particles. This can be attributed to the difference in porosity between the bone types (see Table 2).

### *Calculation of the diffusivities using Fick's law*

Using the least-squares method a straight line was fitted through the data points of Figure 4. The slope of this line, $K_F$, is given in Table 4. Using Eq. 8, the effective diffusivities of HCl are calculated. In Figure 5 the effective diffusivities are plotted vs. the concentration at $t = 0.5$ h. Although the rate of demineralization increases with increasing concentration (Table 4), the diffusivity decreases with increasing concentrations. It is known from the literature that the diffusivity depends on the viscosity of the solution (van der Wielen et al., 1997; Versteeg and Swaaij, 1983), but the increase of viscosity is too low to cause this decrease of diffusivity. This means that other factors besides the concentration gradient of HCl become more important in the mass transfer. Higher concentrations of HCl will give higher concentrations of $Ca(H_2PO_4)_2$ and $CaCl_2$. This means that HCl encounters more frictional forces when it is diffusing into the demineralized layer. Friction forces are not taken into account in these calculations of the effective diffusivities. The demineralization rate can thus not be predicted with Fick's law without doing the demineralization experiments.

Figures 5a–5d also show the influence of temperature on the diffusivity. In all cases the diffusivity increases with increasing temperature. There are different relations to describe this temperature dependency of the diffusivity (Reid et al., 1987): most of them are based on the Stokes–Einstein relation in which the diffusivity is directly proportional to the temperature divided by the viscosity (which is also a function of temperature).

### *Describing the demineralization with Maxwell–Stefan equations*

The fluxes, concentrations, and the electrical potential gradient are calculated for all bone types at 0.5, 3, and 6 wt % HCl, using Eqs. 9–15. In all calculations, the temperature was set at 15°C. The calculations, which were done at different values of $\Delta s$, showed that the molar fractions and the electrical potential gradient are not dependent on $\Delta s$ but only on the HCl concentration in the bulk liquid. The parameter $K_{MS}$ is thus dependent only on the HCl concentration. Figures 6 and 7 show the situation around the demineralized layer at different concentrations of HCl for bone types II–IV.

Equation 17 was used to calculate the penetration depth as a function of time. Figure 8 shows a parity plot of the penetration depth obtained by Eq. 17 and the experimental penetration depth. The predicted and experimental values are in good agreement but have a slight systematic error. This may be attributed to the change in flexibility of the collagen chains in the demineralized zone during deminer-

**Table 5. $K$-Values Compared to the $K$-Value at 6 wt % HCl at Different HCl Concentrations Found by the Maxwell Stefan Model, $K_{MS}$ and by the Experimental Data, $K_F$**

| Bone Type | $C_{HCl}$ (wt %) | $K_{MS}(C_{HCl})/K_{MS}(6)$ | $K_F(C_{HCl})/K_F(6)$ |
|---|---|---|---|
| II | 0.5 | 0.4 | 0.4 |
| II | 3 | 0.8 | 0.8 |
| II | 6 | 1 | 1 |
| IV | 3 | 0.8 | 0.8 |
| IV | 6 | 1 | 1 |

alization. Although the predicted values for the penetration depth are slightly too high, the Maxwell–Stefan model predicts very well the change in demineralization rates at different HCl concentrations. The increase in $K_{MS}$ at higher HCl concentrations is the same as the experimentally found increase of $K_F$ as shown in Table 5. The increase is caused by the increase of HCl concentration, but would have been much higher if there was no increase in friction force. The increase in friction force is caused by the increase in product concentrations in the demineralized layer (Figures 6 and 7). The description of the demineralization process with Fick's law does not take this increase into account. Therefore, the calculated effective diffusivity has to decrease at higher HCl concentrations to compensate for this failure.

## Conclusion

The penetration depth of HCl into animal bone particles as a function of time is measured at different concentrations of HCl and at different temperatures. The results showed that an increase in either temperature or concentration gives an increase in the demineralization rate. The results were used to calculate an effective diffusivity of HCl in animal bone using Fick's law. It was found that the effective diffusivity increases with increasing temperatures but decreases with increasing concentrations. This decrease in effective diffusivity cannot easily be predicted, which makes Fick's law unsuitable for an accurate prediction of the demineralization rate.

With the Maxwell–Stefan model, it is possible to predict the demineralization process more accurately. It takes into account the friction between the ions and between the ions and the matrix and between the ions and water. The model results are in good agreement with the experimental data. A higher proton concentration gives a higher concentration of all the ions, which results in higher friction forces between the ions. This will slow down the increase in diffusion rate of the protons at higher HCl concentration.

## Notation

$c$ = total concentration
$C_{HCl}$ = concentration of HCl
$d_p$ = diameter of bone particle
$D$ = Fick's diffusivity
$Đ$ = Maxwell–Stefan diffusivity
$Đ^{\infty}_{+w}$ = intrinsic diffusivity of a cation in water
$Đ^{\infty}_{-w}$ = intrinsic diffusivity of an anion in water
$Đ_{ij}$ = diffusivity of component $i$ in $j$
$F$ = Faraday constant
$J_{HCl}$ = flux of HCl
$K$ = constant
$N_i$ = molar flux of component $i$
$r$ = distance in bone particle from surface
$R$ = gas constant
$r_c$ = unreacted core radius
$r_f$ = radius of collagen fiber
$r_I$ = radius of ion $i$
$r_P$ = radius of bone particle
$t$ = time
$T$ = temperature
$x_I$ = molar fraction of component $i$
$z_I$ = charge number $i$

### Greek letters

$\beta_i$ = stoichiometric coefficient
$\phi$ = electrical potential
$\lambda$ = moles of HCl necessary to demineralize 1 $m^3$ bone
$\eta$ = viscosity
$\phi_f$ = volume fraction of fibers
$\Delta s$ = thickness of demineralized layer

### Subscripts and superscripts

F = Fick
MS = Maxwell–Stefan
S = solid phase
L = liquid phase
G = gas state

## Literature Cited


Babel, W., D. Schulz, M. Giesen-Wiese, U. Seybold, H. Gareis, E. Dick, R. Schrieber, A. Schott, and W. Stein, "Gelatin," *Ullmann's Encyclopedia of Industrial Chemistry*, 6th Edition, Electronic Release (2000).

Bosma, J. C., and J. A. Wesselingh, "Partitioning and Diffusion of Large Molecules in Fibrous Structures," *J. Chromatogr. B*, **743**, 169 (2000).

Croome, R. J., and F. G. Clegg, *Photographic Gelatin*, The Focal Press, New York (1965).

Levenspiel, O., *Chemical Reaction Engineering*, 2nd Edition, Wiley, New York (1972).

Makarewicz, P. J., P. J. Harasta, and S. L. Webb, "Kinetics of Acid Diffusion and Demineralization of Bone," *J. Photographic Sci.*, **28**, 177 (1980).

Mills, R., and V. V. M. Lobo, *Self-Diffusion in Electrolyte Solutions*, Elsevier, Amsterdam (1989).

Reid, R. C., J. M. Prausnitz, and B. E. Poling, *The Properties of Gases and Liquids*, 4th Edition, McGraw-Hill, New York (1987).

Rose, P. I., "Gelatin," *Encyclopedia of Polymer Science and Engineering*, 2nd Edition, Wiley, New York, Vol. 7, pp. 488–513 (1987).

van der Wielen, L. A. M., M. Zomerdijk, J. Houwers, and K. Ch. A. M. Luyben, "Diffusivities of Organic Electrolytes in Water," *Chem. Eng. J.*, **66**, 111 (1997).

Versteeg, G. F., and W. P. M. van Swaaij, "Solubilities and Diffusivities of Acid Gases ($CO_2$, $N_2O$) in Aqueous Alkanilamine Solutions," *J. Chem. Eng. Data*, **33**, 29 (1988).

Werten, M. W. T., T. J. van den Bosch, R. D. Wind, H. Mooibroek, and F. A. de Wolf, "High-Yield Secretion of Recombinant Gelatins by *Pichia pastoris*," *Yeast*, **15**, 1087 (1999).

Werten, M. W. T., W. H. Wisselink, T. J. van den Bosch, E. C. de Bruin, and F. A. de Wolf, "Secreted Production of a Custom-Designed, Highly Hydrophilic Gelatin in *Pichia pastoris*," *Protein Eng.*, **14**, 447 (2001).

Wesselingh, J. A., and R. Krishna, *Mass Transfer in Multicomponent Mixtures*, 1st edition, Delft University Press, Delft, Netherlands (2000).

Wesselingh, J. A., P. Vonk, and G. Kraaijeveld, "Exploring the Maxwell–Stefan Description of Ion Exchange," *Chem. Biochem. Eng. J.*, **57**, 75 (1995).

Westerterp, K. R., W. P. M. van Swaaij, and A. A. C. M. Beenackers, *Chemical Reactor Design and Operation*, 2nd Edition, Wiley, New York (1987).



*Manuscript received Nov. 12, 2003, and revision received Feb. 27, 2004.*